Article

A Machine Learning Approach for Predicting Black Hole Mass in Blazars Using Broadband Emission Model Parameters

Krishna Kumar Singh [1,2,*], Anilkumar Tolamatti [1,2], Sandeep Godiyal [1], Atul Pathania [1] and Kuldeep Kumar Yadav [1,2]

1   Astrophysical Sciences Division, Bhabha Atomic Research Centre, Mumbai 400085, India
2   Homi Bhabha National Institute, Anushakti Nagar, Mumbai 400094, India
*   Correspondence: kksastro@barc.gov.in

Abstract: Blazars are observed to emit non-thermal radiation across the entire electromagnetic spectrum from the radio to the very-high-energy γ-ray region. The broadband radiation measured from a blazar is dominated by emission from a relativistic plasma jet which is assumed to be powered by a spinning supermassive black hole situated in the central region of the host galaxy. The formation of jets, their mode of energy transport, actual power budget, and connection with the central black hole are among the most fundamental open problems in blazar research. However, the observed broadband spectral energy distribution from blazars is generally explained by a simple one-zone leptonic emission model. The model parameters place constraints on the contributions from the magnetic field, radiation field, and kinetic power of particles to the emission region in the jet. This in turn constrains the minimum power transported by the jet from the central engine. In this work, we explore the potential of machine learning frameworks including linear regression, support vector machine, adaptive boosting, bagging, gradient boosting, and random forests for the estimation of the mass of the supermassive black hole at the center of the host galaxy of blazars using the best-fit emission model parameters derived from the broadband spectral energy distribution modeling in the literature. Our study suggests that the support vector machine, adaptive boosting, bagging, and random forest algorithms can predict black hole masses with reasonably good accuracy.

Keywords: machine learning; blazars; non-thermal radiation; black holes

1. Introduction

Modern astronomy suggests that most of the galaxies in the universe host supermassive black holes (SMBHs; $10^6 M_\odot$–$10^9 M_\odot$) in their central region. The SMBHs are expected to play a lead role in the formation and evolution of the host galaxies throughout cosmic time [1]. A large fraction of such galaxies have been identified as having active galactic nuclei (AGN), which are highly energetic and non-explosive astrophysical sources, and exhibit unique observational features over the entire electromagnetic spectrum. Radiation emission from AGNs is connected to the actively accreting central SMBHs and is unrelated to the stellar emission powered by nuclear fusion. According to the unified model, AGNs mainly consist of an accretion disk around the SMBH, fast moving gas clouds in the vicinity of the SMBH, called the broad line region (BLR), a dusty torus surrounding the BLR and a slowly moving gas named the narrow line region [2–4]. A most extreme class of AGN, called blazars, exhibit a pair of oppositely oriented jets with one of them propagating close to the line of sight of the observer on Earth. These jets are radio-loud, highly collimated, powerful, relativistic, outflows of magnetized plasma and transport energy and momentum to large scales [5]. They emanate from the central region in the vicinity of SMBH and are perpendicular to the accretion disc or along the rotation axis of the black hole [6–8]. The energy transport in blazar jets in the form of bulk motion of leptons, hadrons, and magnetic field is powered by the central engine. However, the exact form of energy (ordered kinetic

energy of plasma and/or Poynting flux) transportation in the jets is still not known. It is generally understood that the sources of the jets share common properties of the presence of a central compact object surrounded by an accretion disk and a large scale magnetic field with a favorable topology [6,9–11]. According to theoretical models and evidence obtained from high-resolution radio imaging, the relativistic jets in AGNs or blazars are formed when the SMBH spins and accretion disk is strongly magnetized. Thus, the propelling of jets takes place due to the twisting of the magnetic fields by the orbiting accretion disk or differentially rotating ergosphere, where the spin of SMBH drags the inertial frames. Furthermore, the central SMBHs are assumed to shape the jets at very large distance scales; therefore, a reliable measurement of their physical properties including mass is crucial in understanding the black hole jet connection in blazars. Therefore, black hole mass is one out of many parameters that are needed, not only in blazars, but radio galaxies and radio-quiet AGNs as well in order to understand blazars in particular and AGNs in general.

Most of the information about jets is available from the multi-wavelength observations in the radio, optical, X-ray, and gamma-ray bands. The special geometrical situation of blazar jets causes the non-thermal jet emission to be strongly amplified by the Doppler beaming effect and dominant at all wavelengths [12]. They also exhibit extreme observational characteristics such as variability at different timescales in all wavebands, strong and variable degrees of optical polarization, superluminal motion in radio, and harder-when-brighter behavior in gamma rays [13,14]. Therefore, the observed features of electromagnetic radiation in different wavebands can be used as a potential probe for the physical properties of the emission zone in the jet and also the SMBH. As the direct kinematic observation of the mass of black holes in the blazars is limited by finite spatial resolution, less direct and more indirect methods have been devised for estimating the mass of SMBHs [15]. One set of less direct methods is based on the assumption that the BLR-SMBH is a virial system and the mass of a black hole can be estimated from the orbital radius and the Doppler velocity [16–18]. Among the less direct methods, the reverberation mapping technique derives the distance of the BLR from the black hole by utilizing the time-lag between continuum and emission lines [19]. Since reverberation mapping is a very laborious technique, a relatively simpler alternative is the estimation of the size of BLR from the ultraviolet/optical luminosity [20,21]. It is important to note here that the optical spectra of a particular class of blazars, called BL Lac objects or BL Lacs, are devoid of strong emission lines and exhibit only weak or no spectral lines. These sources are also unified as low-excitation radio galaxies which exhibit radiatively inefficient accretion but produce collimated jets very efficiently [4,22]. The weak -or no-lined nature of the BL Lacs type of blazars introduces challenges for the reliable estimation the black hole mass using reverberation mapping as they lack the presence of BLR. Even if weak emission lines are detected from a few BL Lacs, the estimated black hole mass will be unreliable unless Doppler boosting is applied to the continuum luminosity [23]. Thus, a different technique is required for measuring the central SMBH mass black hole in BL Lacs. In an alternative approach, dynamics of the stars near the center of AGN is utilized for weighing the black hole mass. This method is based on the empirical correlations between the black hole mass and line-of-sight stellar velocity dispersion if the host galaxy of the AGN can be decomposed from the central region [24–26]. It is important to stress that the observed correlation between black hole mass and stellar velocity dispersion weakly evolves with redshift in the local universe [27]. Furthermore, it can be different for blazars than for low-redshift AGNs (most likely jetless), since stellar velocities are affected differently by jets emitting non-thermal radiation and thermal radiation from the accretion disk. A sizable sample of black hole masses has been estimated for BL Lacs type of blazars using the luminosity of their host galaxies [28]. However, the correlation between black hole mass with host galaxy luminosity is not as tight as that of the stellar velocity dispersion. The black hole masses for more than 700 BL Lacs have been derived using correlation with the stellar velocity dispersions [23].

In the indirect approach, variability features observed in the multi-wavelength light curves of blazars are used to estimate the SMBH mass. An empirical anticorrelation between

the variability amplitude in X-ray band and black hole mass is found to be a better black hole mass estimator than the virial methods discussed above [29,30]. A correlation between photon spectral index and luminosity in the X-ray band is used to determine the mass of SMBH in blazars [31,32]. The observed X-ray luminosities alone are also used to estimate the masses of central SMBHs [33]. The intra-day variability present in the optical data of blazars gives a crude estimation of the central SMBH masses [34,35]. Spectropolarimetric observations of the broad emission lines and their polarization characteristics allow for the measurement of the SMBH mass using single epoch observations [36]. In this work, we report the application of various machine learning algorithms to estimate the central SMBH mass in blazars using the best fit physical parameters, which have been derived from the broadband emission modeling. This method takes into account the near-simultaneous and time-averaged flux measurements in all wavebands over the whole electromagnetic spectrum to predict the SMBH mass for a given blazar. It can be applied to all type of blazars or AGNs whose broadband emission modeling is possible with a set of non-thermal model parameters. Therefore, this method is free from the limitations of various approaches for black hole mass measurements as described above. Determination of black hole mass for a large number of blazars would help in understanding the statistical properties of relativistic jets, estimating if the black hole or another parameter is the main driver of non-thermal emission from jets and the scaling of relativistic jets with mass of SMBHs. An accurate estimation of black hole mass will also help in optimization of the parameters of a physical model describing the jet emission. It is also used to set an approximate upper limit to AGN energetics via the Eddington limit. The most unique aspect of the machine learning approach reported in the present work relies on the fact that it only depends on the model parameters involved in the modeling of broadband non-thermal jet emission. The structure of paper is the following. In Section 2, broadband emission models for blazars are briefly discussed. The data sample of blazars used in the present work is described in Section 3. The description of different machine learning algorithms employed for SMBH mass estimation is given in Section 4. Results are discussed in Section 5, and finally we conclude the study in Section 6.

2. Broadband Emission from Blazars

Blazars are dominant source of broadband electromagentic radiation in the extragalactic universe. The intensity from these sources is greatly boosted in the observer frame due to strong relativistic beaming effects and is dominated by non-thermal continuum emission originating within the jet. A fractional dissipation of power carried by relativistic plasma jets of blazars results in the emission of beamed radiation that is observed on Earth [37]. The measured characteristic spectral energy distributions (SEDs) of blazars, consisting of two broad humps, have been successfully reproduced by a simple one-zone leptonic model [12,38]. The first hump, peaking at low energy in the IR-optical-UV band, is well attributed to the synchrotron emission by relativistic electrons from a compact region permeated in tangled magnetic field inside the jet. The second hump peaks at high energy in the GeV-TeV gamma-ray band and is described by the inverse Compton (IC) scattering of low-energy seed photons by the relativistic electrons in the jet [39,40]. If the target photons for IC process are the synchrotron photons itself, it is referred to as the synchrotron self-Compton (SSC) model for high energy gamma-ray emission [41,42]. On the other hand, if the population of seed photons is described by an external radiation field originating from the accretion disk [43], the broad-line region [44,45] or the dusty torus [46,47] is known as the external Compton (EC) model. A qualitative description of the simple one-zone synchrotron and IC models adopted for broadband SED modeling of blazars used in the present work is in the following [37].

The emission region, a spherical blob of radius R, is located at a distance R_{diss} from the central SMBH of mass M_{BH}. The emission zone is moving relativistically with a velocity of βc (c is the speed of light in vacuum) corresponding to a bulk Lorentz factor Γ. The total

power injected into the emission region in the form of relativistic electrons in the co-moving frame is given by

$$P_i' \; = \; V \, m_e c^2 \int \gamma \, Q(\gamma) \, d\gamma \tag{1}$$

where $V = 4\pi \, R^3/3$ is the volume of emission zone, $\gamma m_e c^2$ is the relativistic energy of an electron, and $Q(\gamma)$ is the injection rate of the primary electrons. The injection function of relativistic electrons is a smooth broken power law in the form:

$$Q(\gamma) \; = \; Q_0 \, \frac{(\gamma/\gamma_b)^{-s_1}}{1 + (\gamma/\gamma_b)^{s_2 - s_1}} \tag{2}$$

where s_1 and s_2 are the power law spectral indices before and after the break energy γ_b. The energy distribution $N(\gamma)$ of the particles in the emission region is obtained by solving the continuity equation by taking into account the particle injection, radiative cooling, and $e^- $-$e^+$ pair production due to photon–photon collision. The injection process is assumed to last for a light crossing time of R/c and $N(\gamma)$ is calculated at this time. The magnetic energy density in the emission region is given by $U_B \; = \; B^2/8\pi$, where B is the strength of tangled magnetic field. Assuming a steady-state electron energy distribution $N(\gamma)$, emissions due to the synchrotron, SSC, and EC processes are calculated. The total observed flux is given by

$$F_{obs}(\nu_{obs}) \; = \; \frac{\delta^3 \, (1+z) \, V}{d_L^2} \left(I_{syn}(\nu) + I_{SSC}(\nu) + I_{EC}(\nu) \right) \tag{3}$$

where $\nu_{obs} \; = \; \nu \, \delta/(1+z)$ is the observed photon frequency corresponding to the co-moving photon frequency ν, δ is the Doppler factor, z is the redshift of the source, d_L is the luminosity distance, and I is the intensity corresponding to the associated radiative process. The BLR is assumed to have a shell-type structure located at distance

$$R_{BLR} \; = \; 10^{17} \left(\frac{L_d}{10^{45}} \right)^{1/2} \; \text{cm} \tag{4}$$

where L_d is the luminosity of accretion disk. The total power carried by jet or jet luminosity (L_j) includes radiated power, Poynting flux corresponding to the magnetic field, power in bulk motion of emitting electrons, and power in the bulk motion of cold protons (assuming one proton at rest per emitting electron). A detailed description of the model can be found in [37].

3. The Data Sample of Blazars

Ghisellini et al. (2010) have studied the entire sample of blazars of known redshift detected by the Large Area Telescope onboard the *Fermi* satellite (Fermi-LAT) during its first three months of operation [48]. They have selected 85 blazars with reasonable data coverage of their broadband SEDs from optical to gamma rays. Sources in the sample were in the average state. The optical/UV measurements were used to segregate the contribution due to accretion disk from the non-thermal jet emission of the selected blazars. The leptonic one-zone model, described in Section 2, was employed to reproduce the observed multi-wavelength emission of the blazars. The time-averaged broadband SEDs in the sample are described by different radiative cooling by the relativistic electrons in the emission region with lower power jets containing higher energy electrons. The seed photons for EC process to produce gamma-ray photons were provided by BLR. The fitting results indicate that all blazars in the sample have small viewing angles with the relativistic jet pointing towards the Earth. Assuming that the mass of the SMBH plays an important role in the measured broadband SED, we have selected 60 out of the 85 blazars reported by Ghisellini et al. (2010) [48] for use in the present study. Our selection is based on the criteria that all model parameters including mass of black holes should be available for the sample of blazars. Among the various model parameters reported in the literature, we have z, R_{diss}, R_{BLR}, P_i',

B, Γ, γ_b, γ_{max} (maximum Lorentz factor of injected electrons), s_2, and L_j (total power carried by the jet) as the input parameters for predicting the value of M_{BH} for each blazar in the sample. Distributions of these parameters for the 60 blazar sample are shown in Figure 1. The data sample comprising 60 blazars is randomly divided into training and test data sets. The training data set consists of the parameters of 45 blazars whereas the parameters of the remaining 15 blazars were used as test data for the validation of the methodology for black hole mass prediction based on different machine learning algorithms. The scatter plots of M_{BH} vs. the SED model parameters, reported in Figure 2, do not indicate any definite pattern/correlation. This implies that the black hole mass does not exclusively depend on any of the SED parameters of the blazars. Therefore, we use advanced machine learning tools to estimate the masses of SMBHs in the blazars using broadband emission parameters as inputs.
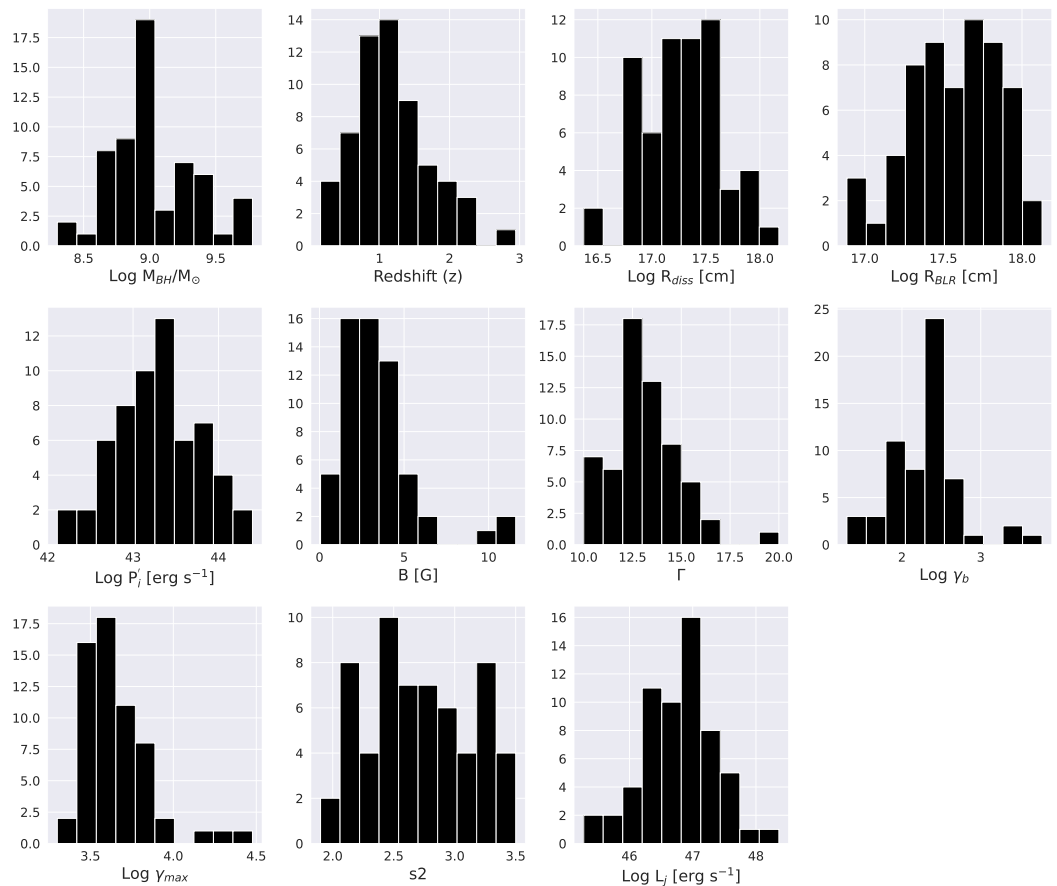

Figure 1. Distribution of best fit model parameters for reproducing the SED of 60 blazars. The data are taken from the literature published in [48].
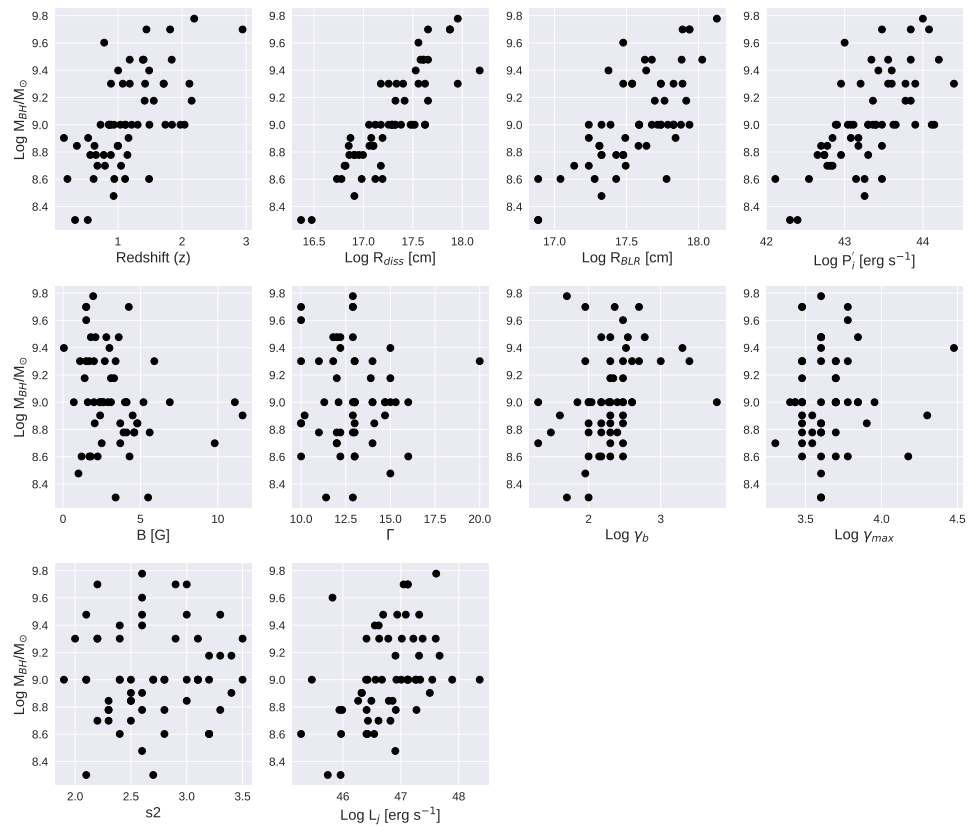
Figure 2. Scatter plots for the mass of SMBH as a function of SED model parameters of the blazar data sample.

4. Machine Learning Algorithms

Machine learning techniques and artificial intelligence have proven to be applicable in broad area of scientific research in astronomy and astrophysics [49–51]. They are widely used for a variety of tasks such as the detection, characterization, classification, and prediction using big astronomical data sets. Machine learning algorithms are generally grouped into two categories, namely supervised and unsupervised. Supervised algorithms learn over time from a training data set based on correct input–output pairs provided by experts and then yield the expected output. Different learning models, algorithms, and computational techniques are employed in supervised machine learning. In unsupervised machine learning algorithms, models are trained using unlabeled data and learn from the hidden patterns/complex relationships in the given data set to estimate the output. In this work, we used the data set described in Section 3 and employed the following six supervised machine learning algorithms to predict the masses of SMBHs in blazars.

4.1. Linear Regression

Linear regression is a simple and popular statistical method for the predictive analysis. It fits a linear model between a dependent variable (output) and one or more independent variables (inputs) with appropriate weights or coefficients of lines. A cost function optimizes the weights or regression coefficients by minimizing the residual sum of least squares between the outputs in training data set and predicted outputs by the linear approximation.

4.2. Support Vector Machine

A support vector machine (SVM) algorithm is used for both regression and classification and regression problems. It creates the best line or decision boundary that can separate higher-dimensional space into classes so that a new data point may be associated with a correct category. The best decision boundary is referred to as the hyperplane, where

the distance between two classes of data points is the maximum. The dimensions of the hyperplane depends on the features present in the data set and the extreme data points or vectors close to hyperplane are termed as support vectors. This offers a very high accuracy when compared to linear regression algorithms. The SVM algorithm is implemented using a kernel, which transforms an input data set into the required form. In the present work, we have used a radial basis function kernel with $C = 10$ and $\gamma = 0.01$ as parameters.

4.3. Adaptive Boosting

Boosting algorithms in machine learning are based on a model built using a training data set followed by a second model to rectify the errors developed in the first model. The procedure is continuously applied unless the errors are minimized and the output is predicted correctly. The adaptive boosting (AdaBoost) algorithm is used as an ensemble method in machine learning. In this technique, a model is built and equal weights are assigned to all the data points. Higher weights are assigned to incorrectly predicted data points. In the next model, points with higher weights are given more importance. It continuously trains models unless the error is minimized. Boosting is used to reduce the bias and the variance. The AdaBoost technique essentially works on the principle of learners growing sequentially.

4.4. Bagging

Bagging, also known as bootstrap aggregating, is an improved ensemble learning technique which combines several models to decrease the variance and avoid overfitting. Bagging is based on the key idea that multiple base learners trained separately with a random sample from the training data set through a voting or averaging approach produce more stable and accurate model [52].

4.5. Gradient Boosting

Unlike AdaBoost, the weights of training datasets are not tweaked in the gradient boosting algorithm. Each predictor is trained using the residuals of the predecessor as labels. It calculates the gradient for optimization of a given cost function. The key idea is based on minimizing the residuals of each learner base in a sequential manner. Each base learner added to the sequence minimizes the residuals determined by the previous learner. This is repeated until the error function is approximately zero or a specified number of base learners is completed [53].

4.6. Random Forest

Random forest is a flexible algorithm which is widely used as an ensemble technique in both classification and regression problems. The term forest refers to a collection of uncorrelated decision trees merged together to reduce variance and create accurate data predictions. It takes into account the prediction from each tree on the basis of majority votes of the predictions, instead of relying on single decision tree to predict the final output. A higher number of trees in the forest leads to better accuracy and prevents overfitting. The random forest algorithms works in two phases: first, the random forest is created by combining multiple decision trees and second, predictions are made for each tree created in the first phase [54]. Compared to other machine learning algorithms, random forest takes less training time and very efficiently predicts output with high accuracy.

5. Results and Discussion

We take advantage of the availability of a large set of model parameters for broadband emission from 60 blazar jets and measurements of the masses of respective SMBHs as described in Section 3. The blazar sample data set is split into training and testing sets with a ratio of 25%. Hence, the emission model parameters z, R_{diss}, R_{BLR}, P'_i, B, Γ, γ_b, γ_{max}, s_2, and L_j of 45 blazars are provided as the inputs for the six machine learning algorithms mentioned in Section 4 to predict M_{BH} from the *scikit-learn*. The performance of model

corresponding to the training data set is evaluated on the basis of two loss functions, namely root-mean square error (RMSE) and goodness of fit, given by R^2. The RMSE between the desired and predicted outputs gives outliers a large weight and needs to be minimized during the training process. R^2, also known as the coefficient of determination, is a statistical measure of the scatter of data points around the fit regression line. The values of RMSE and R^2 corresponding to the six machine learning algorithms are shown in Figure 3. A comparison of RMSE for different algorithms suggests that the AdaBoost gives the minimum RMSE value of $\sim$0.1, followed by SVM, bagging, and random forest. Similarly, $R^2 \geq 0.8$ values were obtained for AdaBoost, SVM, bagging, and random forest algorithms with a maximum value of $R^2 = 0.87$ for AdaBoost. For a given data set, a higher value of R^2 indicates smaller differences between the desired and predicted outputs. Therefore, the loss functions RMSE and R^2 suggest that among the six algorithms applied in the present work, AdaBoost is the best performing technique, followed by SVM, bagging, and random forest.

Therefore, we have used the better performing algorithms AdaBoost, SVM, bagging, and random forest to predict the M_{BH} values for 15 blazars in the test data set. The predicted vs. true values for these algorithms are reported in Figure 4. It is observed that all the four algorithms predict the M_{BH} values reasonably well, as the predicted and desired values are almost linearly correlated. We have also estimated the relative importance of various input parameters in predicting the masses of SMBHs. The results shown in Figure 5 imply that the location of the emission zone in the blazar jet (R_{diss}) is the most important parameter in predicting the values of M_{BH}. The second important input parameter is the bulk Lorentz factor (Γ) of the emission zone in the case of SVM and random forest algorithms. The location of emission region controls the radiative cooling processes in the blazar emission models. However, the dominant mechanism for non-thermal emission at high energy and location of emission zones remain poorly understood [55]. The complicated nature of blazars has resulted in a large number of proposals on the location of emission zone in the jets. Sample of blazars have been observed to have a high bulk Lorentz factor or Doppler factor and show a positive correlation between M_{BH} and Γ [56]. Therefore, the exact determination of R_{diss} using high-resolution future instruments and Γ measurements will help in the better prediction of M_{BH} for blazars using the machine learning-based methodologies as discussed in this study. A recent study of a large sample of blazars suggests a significant correlation between jet kinetic power and the spin of SMBH [57]. The spin of black holes and accretion are found to be the dominant contributors to the jet kinetic power. This indicates that blazar jet power depends on the mass of black hole. In another study, a strong relation between bulk Lorentz factors and black hole mass is also reported [58]. These results suggest that the Blandford–Znajek mechanism [6] plays a leading role in jet formation and acceleration in blazars. Therefore, the results obtained in the present study will help ito better understand jet formation in blazars as well as jetted AGNs, which are open issues in astrophysics research.

Although steady state single-zone leptonic models have been successful in providing acceptable fits for the SEDs of almost all classes of blazars, they face several theoretical and observational challenges as they sometimes demand unusual values of the physical parameters [59,60]. Very fast variability during flaring episodes and the occurrence of orphan TeV flares pose challenges to the time-dependent implementations of one-zone leptonic models [61–63]. Furthermore, the nature of emitting plasma in the blazar jets still remains unclear and hadronic models and lepto-hadronic models have began to receive widespread acceptance [12]. The discovery of very-high-energy neutrinos in 2013 by the IceCube experiment and their plausible association with the gamma-ray flaring episode of a blazar challenges the leptonic models and supports the role of hadronic models for blazar emission [64,65]. In order to explain some of the observational findings, two-zone leptonic models and several variations of the multi-zone models have also been proposed as the number of relevant emission zones is unknown [66,67]. Therefore, the results derived in the present work using single zone leptonic models may not be purely realistic. This study only explores the potential

of machine learning applications for black hole mass estimation using broadband emission model parameters. However, it can be applied to the more complex models, as described above, if SED model parameters are available for a large number of blazars in future.
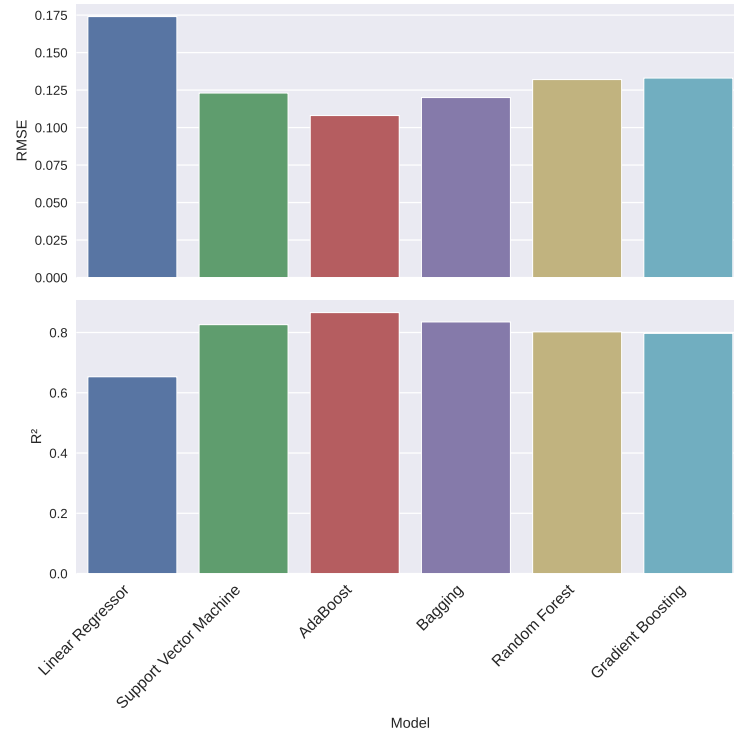

Figure 3. RMSE and R^2 estimations for different machine learning algorithms using the training data set.
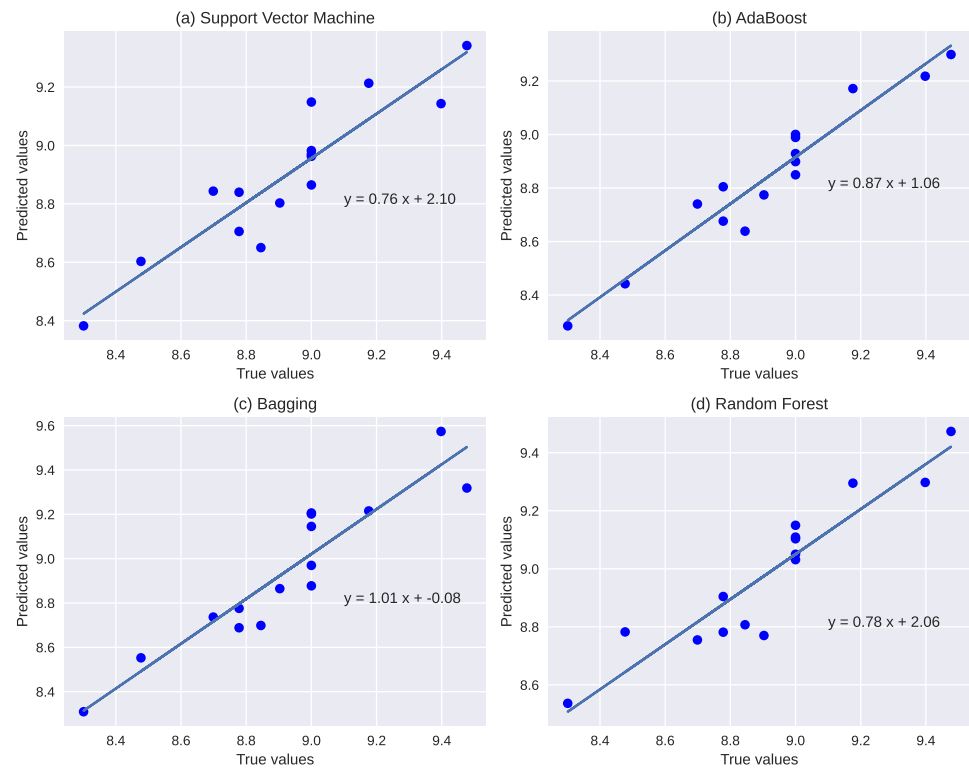

Figure 4. Predicted and true values of M_{BH} for 15 blazars in the test data set.
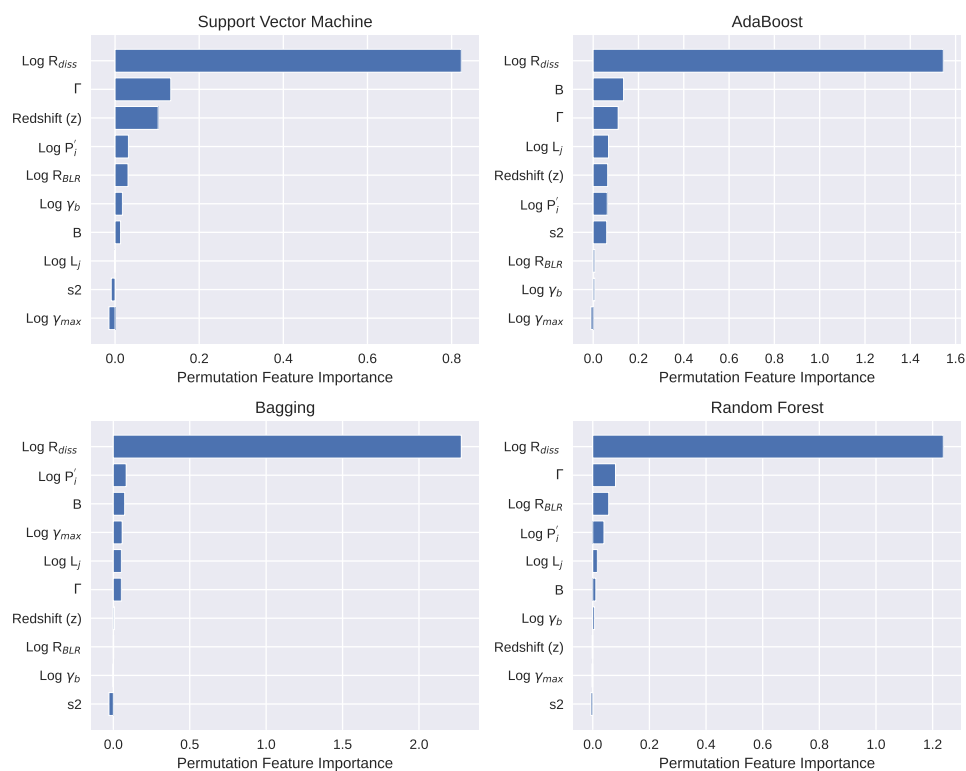
Figure 5. Relative importance of various input parameters for different machine learning algorithms.

6. Conclusions

The broadband observations of blazars are found to play a leading role in determining the physical properties of the central SMBH in the host galaxies as well as the relativistic jets. Many methods have been developed in the literature to estimate the mass of SMBH for blazars using the measurements of electromagnetic radiation from jets. In this work, we have explored the potential application of machine learning algorithms for the estimation of the masses of SMBHs in blazars. The main findings of this study are:

- Blazars, being bright sources across the electromagnetic spectrum, are visible over large cosmological distances. Therefore, the physical properties of the central SMBHs are important in mapping the structure formation and evolution in the early universe.
- The best fit parameters of the blazar SEDs, derived under the framework of a simple, homogeneous, one-zone leptonic emission model, can be effectively utilized to estimate the mass of SMBHs in blazars.
- Out of the six machine learning algorithms used in this work, AdaBoost, SVM, bagging, and random forest are found to give consistent performance for predicting the mass of SMBH using broadband SED model parameters as inputs.
- A very strong linear correlation is observed between the predicted and desired masses of the SMBHs for the blazar sample used in the present work. The predictions by different machine learning algorithms have very good accuracy.
- Among the several model parameters for blazar emission, location of emission zone from the central region and bulk Lorentz factor of the jet are the crucial parameters for predicting the mass of SMBH. However, more future multi-wavelength observations of blazars are needed to further confirm and validate the findings of this work as the central black hole mass is the driving parameter of the blazar activities.

Author Contributions: K.K.S., Conceptualization and original draft preparation; A.T., data curation and software; S.G., data curation; A.P., data curation; K.K.Y., review and editing. All authors have read and agreed to the published version of the manuscript.

Conflicts of Interest: The authors declare no conflict of interest.

References

1. Kauffmann, G.; Haehnelt, M. A unified model for the evolution of galaxies and quasars. *Mon. Not. R. Astron. Soc.* **2000**, *311*, 576–588. [CrossRef]
2. Urry, C.M.; Padovani, P. Unified Schemes for Radio-Loud Active Galactic Nuclei. *Publ. Astron. Soc. Pac.* **1995**, *107*, 803. [CrossRef]
3. Netzer, H. Revisiting the Unified Model of Active Galactic Nuclei. *Annu. Rev. Astron. Astrophys.* **2015**, *53*, 365–408. [CrossRef]
4. Padovani, P.; Alexander, D.M.; Assef, R.J.; De Marco, B.; Giommi, P.; Hickox, R.C.; Richards, G.T.; Smolčić, V.; Hatziminaoglou, E.; Mainieri, V.; et al. Active galactic nuclei: What's in a name? *Astron. Astrophys. Rev.* **2017**, *25*, 2. [CrossRef]
5. Fabian, A.C. Observational Evidence of Active Galactic Nuclei Feedback. *Annu. Rev. Astron. Astrophys.* **2012**, *50*, 455–489. [CrossRef]
6. Blandford, R.D.; Znajek, R.L. Electromagnetic extraction of energy from Kerr black holes. *Mon. Not. R. Astron. Soc.* **1977**, *179*, 433–456. [CrossRef]
7. Doeleman, S.S.; Fish, V.L.; Schenck, D.E.; Beaudoin, C.; Blundell, R.; Bower, G.C.; Broderick, A.E.; Chamberlin, R.; Freund, R.; Friberg, P.; et al. Jet-Launching Structure Resolved Near the Supermassive Black Hole in M87. *Science* **2012**, *338*, 355–358. [CrossRef]
8. Blandford, R.; Meier, D.; Readhead, A. Relativistic Jets from Active Galactic Nuclei. *Annu. Rev. Astron. Astrophys.* **2019**, *57*, 467–509. [CrossRef]
9. Goldreich, P.; Julian, W.H. Pulsar Electrodynamics. *Astrophys. J.* **1969**, *157*, 869. [CrossRef]
10. Blandford, R.D.; Payne, D.G. Hydromagnetic flows from accretion disks and the production of radio jets. *Mon. Not. R. Astron. Soc.* **1982**, *199*, 883–903. [CrossRef]
11. Lynden-Bell, D. Magnetic collimation by accretion discs of quasars and stars. *Mon. Not. R. Astron. Soc.* **1996**, *279*, 389–401. [CrossRef]
12. Böttcher, M. Progress in Multi-wavelength and Multi-Messenger Observations of Blazars and Theoretical Challenges. *Galaxies* **2019**, *7*, 20. [CrossRef]
13. Singh, K.K.; Meintjes, P.J. Characterization of variability in blazar light curves. *Astron. Nachrichten* **2020**, *341*, 713–725. [CrossRef]
14. Singh, K.K.; Meintjes, P.J.; van Soelen, B.; Ramamonjisoa, F.A.; Vaidya, B. Optical polarization properties of February 2010 outburst of the blazar Mrk 421. *Astrophys. Space Sci.* **2019**, *364*, 88. [CrossRef]
15. Peterson, B.M. Measuring the Masses of Supermassive Black Holes. *Space Sci. Rev.* **2014**, *183*, 253–275. [CrossRef]
16. Krolik, J.H.; Horne, K.; Kallman, T.; Malkan, M.A.; Edelson, R.A.; Kriss, G. Ultraviolet Variability of NGC 5548: Dynamics of the Continuum Production Region and Geometry of the Broad-Line Region. *Astrophys. J.* **1991**, *371*, 541. [CrossRef]
17. Wandel, A.; Peterson, B.M.; Malkan, M.A. Central Masses and Broad-Line Region Sizes of Active Galactic Nuclei. I. Comparing the Photoionization and Reverberation Techniques. *Astrophys. J.* **1999**, *526*, 579. [CrossRef]
18. Krolik, J.H. Systematic Errors in the Estimation of Black Hole Masses by Reverberation Mapping. *Astrophys. J.* **2001**, *551*, 72. [CrossRef]
19. Peterson, B.M. Reverberation Mapping of Active Galactic Nuclei. *Publ. Astron. Soc. Pac.* **1993**, *105*, 247. [CrossRef]
20. Kaspi, S.; Smith, P.S.; Netzer, H.; Maoz, D.; Jannuzi, B.; Giveon, U. Reverberation Measurements for 17 Quasars and the Size-Mass-Luminosity Relations in Active Galactic Nuclei. *Astrophys. J.* **2000**, *533*, 631. [CrossRef]
21. Vestergaard, M. Determining Central Black Hole Masses in Distant Active Galaxies. *Astrophys. J.* **2002**, *571*, 733. [CrossRef]
22. Foschini, L. What We Talk about When We Talk about Blazars. *Front. Astron. Space Sci.* **2017**, *4*, 6. [CrossRef]
23. Plotkin, R.M.; Markoff, S.; Trager, S.C.; Anderson, S.F. Dynamical black hole masses of BL Lac objects from the Sloan Digital Sky Survey. *Mon. Not. R. Astron. Soc.* **2011**, *413*, 805–812. [CrossRef]
24. Ferrarese, L.; Merritt, D. A Fundamental Relation between Supermassive Black Holes and Their Host Galaxies. *Astrophys. J.* **2000**, *539*, L9–L12. [CrossRef]
25. Gebhardt, K.; Bender, R.; Bower, G.; Dressler, A.; Faber, S.M.; Filippenko, A.V.; Green, R.; Grillmair, C.; Ho, L.C.; Kormendy, J.; et al. A Relationship between Nuclear Black Hole Mass and Galaxy Velocity Dispersion. *Astrophys. J.* **2000**, *539*, L13. [CrossRef]
26. Tremaine, S.; Gebhardt, K.; Bender, R.; Bower, G.; Dressler, A.; Faber, S.M.; Filippenko, A.V.; Green, R.; Grillmair, C.; Ho, L.C.; et al. The Slope of the Black Hole Mass versus Velocity Dispersion Correlation. *Astrophys. J.* **2002**, *574*, 740–753. [CrossRef]
27. Shen, Y. The Sloan Digital Sky Survey Reverberation Mapping Project: No Evidence for Evolution in the $M \bullet$-σ_* Relation to z∼ 1. *Astrophys. J.* **2015**, *805*, 96. [CrossRef]
28. Xu, Y.; Cao, X.; Wu, Q. On the BL Lacertae Objects/Radio Quasars and the FR I/II Dichotomy. *Astrophys. J.* **2009**, *694*, L107–L110. [CrossRef]

29. Lu, Y.; Yu, Q. The relationship between X-ray variability and the central black hole mass. *Mon. Not. R. Astron. Soc.* **2001**, *324*, 653–658. [CrossRef]
30. O'Neill, P.M.; Nandra, K.; Papadakis, I.E.; Turner, T.J. The relationship between X-ray variability amplitude and black hole mass in active galactic nuclei. *Mon. Not. R. Astron. Soc.* **2005**, *358*, 1405–1416. [CrossRef]
31. Shemmer, O.; Brandt, W.N.; Netzer, H.; Maiolino, R.; Kaspi, S. The Hard X-ray Spectrum as a Probe for Black Hole Growth in Radio-Quiet Active Galactic Nuclei. *Astrophys. J.* **2008**, *682*, 81–93. [CrossRef]
32. Gu, M.; Cao, X. The anticorrelation between the hard X-ray photon index and the Eddington ratio in low-luminosity active galactic nuclei. *Mon. Not. R. Astron. Soc.* **2009**, *399*, 349–356. [CrossRef]
33. Mayers, J.A.; Romer, K.; Fahari, A.; Stott, J.P.; Giles, P.; Rooney, P.J.; Bermeo-Hernandez, A.; Collins, C.A.; Hilton, M.; Hoyle, B.; et al. Correlations between X-ray properties and Black Hole Mass in AGN: Towards a new method to estimate black hole mass from short exposure X-ray observations. *arXiv* **2018**, arXiv:1803.06891.
34. Gupta, S.P.; Pandey, U.; Singh, K.; Rani, B.; Pan, J.; Fan, J.; Gupta, A. Optical intra-day variability timescales and black hole mass of the blazars. *New Astron.* **2012**, *17*, 8–17. [CrossRef]
35. Zhang, Z.; Gupta, A.C.; Gaur, H.; Wiita, P.J.; An, T.; Gu, M.; Hu, D.; Xu, H. X-ray Intraday Variability of the TeV Blazar Mrk 421 with Suzaku. *Astrophys. J.* **2019**, *884*, 125. [CrossRef]
36. Savić, D.V.; Popović, L.; Shablovinskaya, E. The First Supermassive Black Hole Mass Measurement in Active Galactic Nuclei Using the Polarization of Broad Emission Line Mg II. *Astrophys. J.* **2021**, *921*, L21. [CrossRef]
37. Ghisellini, G.; Tavecchio, F. Canonical high-power blazars. *Mon. Not. R. Astron. Soc.* **2009**, *397*, 985–1002. [CrossRef]
38. Singh, K.K.; Meintjes, P.J.; Ramamonjisoa, F.A. Understanding the giant gamma-ray outburst on June 16, 2015 from the blazar 3C 279. *Astrophys. Space Sci.* **2020**, *365*, 33. [CrossRef]
39. Dermer, C.D. On the Beaming Statistics of Gamma-ray Sources. *Astrophys. J.* **2020**, *446*, L63. [CrossRef]
40. Böttcher, M. Modeling the emission processes in blazars. *Astrophys. Space Sci.* **2007**, *309*, 95–104. [CrossRef]
41. Maraschi, L.; Ghisellini, G.; Celotti, A. A Jet Model for the Gamma-ray—Emitting Blazar 3C 279. *Astrophys. J.* **1992**, *397*, L5. [CrossRef]
42. Tavecchio, F.; Maraschi, L.; Ghisellini, G. Constraints on the Physical Parameters of TeV Blazars. *Astrophys. J.* **1998**, *509*, 608–619. [CrossRef]
43. Dermer, C.D.; Schlickeiser, R. Model for the High-Energy Emission from Blazars. *Astrophys. J.* **1993**, *416*, 458. [CrossRef]
44. Sikora, M.; Begelman, M.C.; Rees, M.J. Comptonization of Diffuse Ambient Radiation by a Relativistic Jet: The Source of Gamma rays from Blazars? *Astrophys. J.* **1994**, *421*, 153. [CrossRef]
45. Fan, Z.; Cao, X.; Gu, M. A Test of External Compton Models for Gamma-ray Active Galactic Nuclei. *Astrophys. J.* **2006**, *646*, 8–15. [CrossRef]
46. Arbeiter, C.; Pohl, M.; Schlickeiser, R. The influence of dust on the inverse Compton emission from jets in Active Galactic Nuclei. *Astron. Astrophys.* **2002**, *386*, 415–426. [CrossRef]
47. Sokolov, A.; Marscher, A.P. External Compton Radiation from Rapid Nonthermal Flares in Blazars. *Astrophys. J.* **2005**, *629*, 52–60. [CrossRef]
48. Ghisellini, G.; Tavecchio, F.; Foschini, L.; Ghirlanda, G.; Maraschi, L.; Celotti, A. General physical properties of bright Fermi blazars. *Mon. Not. R. Astron. Soc.* **2010**, *402*, 497–518. [CrossRef]
49. Baron, D. Machine Learning in Astronomy: A practical overview. *arXiv* **2019**, arXiv:1904.07248.
50. Singh, K.K.; Dhar, V.K.; Meintjes, P.J. An artificial intelligence based approach for constraining the redshift of blazars using γ-ray observations. *Exp. Astron.* **2019**, *48*, 297–311. [CrossRef]
51. Singh, K.K.; Dhar, V.; Meintjes, P. Artificial neural networks for cosmic gamma-ray propagation in the universe. *New Astron.* **2022**, *91*, 101701. [CrossRef]
52. Breiman, L. Bagging Predictors. *Mach. Learn.* **1996**, *24*, 123–140. [CrossRef]
53. Breiman, L. Greedy Function Approximation: A Gradient Boosting Machine. *Ann. Stat.* **2001**, *29*, 5.
54. Breiman, L. Random Forests. *Mach. Learn.* **2001**, *45*, 5–32. [CrossRef]
55. Tolamatti, A.; Ghosal, B.; Singh, K.; Bhattacharyya, S.; Bhatt, N.; Yadav, K.; Chandra, P.; Das, M.; Tickoo, A.; Rannot, R.; et al. Long-term multi-wavelength study of temporal and spectral properties of 3C 279. *Astropart. Phys.* **2022**, *139*, 102687. [CrossRef]
56. Valtaoja, E.; Lindfors, E.; Saloranta, P.M.; Hovatta, T.; Lähteenmäki, A.; Nieppola, E.; Torniainen, I.; Tornikoski, M. Hydrodynamics of Small-Scale Jets: Observational Aspects. *ASP Conf. Ser.* **2008**, *386*, 388–397.
57. Chen, Y.; Gu, Q.; Fan, J.; Zhou, H.; Yuan, Y.; Gu, W.; Wu, Q.; Xiong, D.; Guo, X.; Ding, N.; et al. The Powers of Relativistic Jets Depend on the Spin of Accreting Supermassive Black Holes. *Astrophys. J.* **2021**, *913*, 93. [CrossRef]
58. Zhou, M.; Cao, X.-W. The relation between black hole masses and Lorentz factors of the jet components in blazars. *Res. Astron. Astrophys.* **2009**, *9*, 293. [CrossRef]
59. Begelman, M.C.; Fabian, A.C.; Rees, M.J. Implications of very rapid TeV variability in blazars. *Mon. Not. R. Astron. Soc.* **2008**, *384*, L19–L23. [CrossRef]
60. Costamante, L.; Bonnoli, G.; Tavecchio, F.; Ghisellini, G.; Tagliaferri, G.; Khangulyan, D. The NuSTAR view on hard-TeV BL Lacs. *Mon. Not. R. Astron. Soc.* **2018**, *477*, 4257–4268. [CrossRef]
61. Krawczynski, H.; Hughes, S.B.; Horan, D.; Aharonian, F.; Aller, M.F.; Aller, H.; Boltwood, P.; Buckley, J.; Coppi, P.; Fossati, G.; et al. Multiwavelength Observations of Strong Flares from the TeV Blazar 1ES 1959+650. *Astrophys. J.* **2004**, *601*, 151–164. [CrossRef]

62. Singh, K.K.; Sahayanathan, S.; Sinha, A.; Bhatt, N.; Tickoo, A.; Yadav, K.; Rannot, R.; Chandra, P.; Venugopal, K.; Marandi, P.; et al. A time dependent approach to model X-ray and γ-ray light curves of Mrk 421 observed during the flare in February 2010. *New Astron.* **2017**, *54*, 24–29. [CrossRef]

63. Singh, K.K.; Meintjes, P.; Bisschoff, B.; Ramamonjisoa, F.; van Soelen, B. Gamma-ray and optical properties of the flat spectrum radio quasar 3C 279 flare in June 2015. *J. High Energy Astrophys.* **2020**, *26*, 65–67. [CrossRef]

64. Bissok, M. et al. [IceCube Collaboration]. Evidence for High-Energy Extraterrestrial Neutrinos at the IceCube Detector. *Science* **2013**, *342*, 1242856.

65. Aartsen, M.G.; Ackermann, M.; Adams, J.; Aguilar, J.A.; Ahlers, M.; Ahrens, M.; Alispach, C.; Andeen, K.; Anderson, T.; Ansseau, I.; et al. Characteristics of the Diffuse Astrophysical Electron and Tau Neutrino Flux with Six Years of IceCube High Energy Cascade Data. *Phys. Rev. Lett.* **2020**, *125*, 121104. [CrossRef]

66. Joshi, M.; Böttcher, M. Time-dependent Radiation Transfer in the Internal Shock Model Scenario for Blazar Jets. *Astrophys. J.* **2011**, *727*, 21. [CrossRef]

67. Shukla, A.; Chitnis, V.R.; Singh, B.B.; Acharya, B.S.; Anupama, G.C.; Bhattacharjee, P.; Britto, R.J.; Mannheim, K.; Prabhu, T.; Saha, L.; et al. Multi-frequency, Multi-epoch Study of Mrk 501: Hints for a Two-component Nature of the Emission. *Astrophys. J.* **2015**, *798*, 2. [CrossRef]